Use of Seismic Pavement Analyzer in Pavement Evaluation

SOHEIL NAZARIAN, MARK BAKER, AND KEVIN CRAIN

The Seismic Pavement Analyzer (SPA, patent pending) is an instrument designed and constructed to monitor conditions associated with pavement deterioration. It measures such conditions as voids or loss of support under a rigid pavement, moisture infiltration in asphalt concrete pavement, and delamination of overlays. The SPA detects these types of pavement conditions by estimating Young's and shear moduli in the pavement, base, and subgrade from the following wave propagation measurements: (a) impact echo, (b) impulse response, (c) spectral-analysis-of-surface-waves, (d) ultrasonic-surface-wave-velocity, and (e) ultrasonic-body-wave-velocity. The SPA records the pavement response produced by high- and low-frequency pneumatic hammers on five accelerometers and three geophones. A computer controls data acquisition, instrument control, and interpretation; measurements and interpretations are reported in both screen and data base formats. This paper briefly describes the device and summarizes the usefulness of the equipment in pavement evaluation. The results from several field tests are also discussed. The tests conducted so far have produced very promising results. The device is simple to use, and results have been reliable and repeatable.

In recent years, the focus of pavement engineering has shifted from design and construction of new highways to preventive maintenance and rehabilitation of the existing highways. A highway maintenance program is usually based on a visual condition survey and, to a lesser extent, on appropriate in situ tests. By the time symptoms of deterioration are visible, major rehabilitation or reconstruction is often required. If the onset of deterioration can be measured accurately in the early stages, the problem can often be resolved or stabilized through preventive maintenance.

A relatively inexpensive and precise device for project-level measurements has been developed. This device, the Seismic Pavement Analyzer (SPA, patent pending), can be of help in detecting these types of problems.

OVERVIEW OF SEISMIC PAVEMENT ANALYZER

To diagnose a pavement, mechanical properties of each of the pavement system layers should be determined. The SPA lowers transducers and sources to the pavement and digitally records surface deformations induced by a large pneumatic hammer that generates low-frequency vibrations, and a small pneumatic hammer that generates high-frequency vibrations (see Figure 1).

This transducer frame is mounted on a trailer that can be towed behind a vehicle and is similar in size and concept to a Falling Weight Deflectometer (FWD). The SPA differs from the FWD in that more and higher frequency transducers are used, and more sophisticated interpretation techniques are applied. The SPA is controlled by an operator at a computer connected to the trailer by a cable. The computer may be run from the cab of the truck towing the SPA or from various locations around the SPA.

All measurements are spot measurements; that is, the device has to be towed and situated at a specific point before measurements can be made. A complete testing cycle at one point takes less than 1 min. A complete testing cycle includes situating at the site, lowering the sources and receivers, making measurements, and withdrawing the equipment. During this 1 min, most of the data reduction is also executed.

The SPA collects two levels of data. The first level is raw data. These are the waveforms generated by hammer impacts and collected by the transducers. The second level is processed data. These are pavement layer properties derived from the raw data through theoretical models.

DESCRIPTION OF MEASUREMENT TECHNOLOGIES

Impulse-Response (IR) Method

Two parameters are obtained with the IR method—the shear modulus of subgrade and the damping ratio of the system. These two parameters characterize the existence of several distress precursors. In general, the modulus of subgrade can be used to delineate between good and poor support. The damping ratio can distinguish between the loss of support or weak support. The two parameters are extracted from the flexibility spectrum measured in the field. An extensive theoretical and field study (*1*) shows that except for thin layers (less than 75 mm) and soft paving layers (i.e., flexible pavements), the modulus obtained by the IR method is a good representation of the shear modulus of subgrade. In other cases, the properties of the pavement layers (AC and base) affect the outcome in such a manner that the modulus obtained from the IR test should be considered an overall modulus.

The IR tests use the low-frequency source and geophone G1 (see Figure 1). The pavement is impacted to couple stress wave energy in the surface layer. At the interface of the surface layer and the base layer, a portion of this energy is transmitted to the bottom layers, and the remainder is reflected back into the surface layer. The load and displacement time histories are simultaneously recorded and are transformed to the frequency domain using a Fast-Fourier Transform algorithm. The ratio of the displacement and load (termed flexibility) at each frequency is then determined.

A typical flexibility spectrum is shown in Figure 2(*a*). The response is as expected, except for frequencies below approximately 50 Hz. The erratic nature of the signal at low frequencies is probably because of the movement of the trailer. This problem has been solved in the new design.

The Center for Geotechnical and Highway Materials Research, The University of Texas at El Paso, El Paso, Tex. 79968.

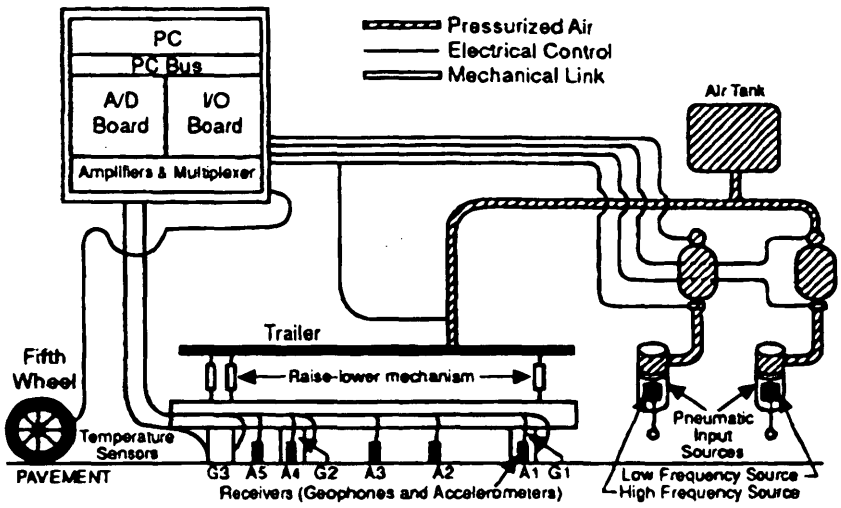

FIGURE 1 Schematic of seismic pavement analyzer.

The coherence function associated with this record is shown in Figure 2(*b*). The coherence values are close to unity except at low frequencies. A coherence value of unity corresponds to a highly coherent signal between the load cell and receiver. In other words, there was no incoherent background noise in the signals.

To determine the modal parameters (static flexibility and damping ratio), a curve is fitted to the flexibility spectrum according to an elaborate curve-fitting algorithm that uses the coherence function as a weighing function. A typical fitted curve is shown in Figure 2(*a*). The agreement between the measured and the fitted data is good. However, once again, because of a lack of quality data at low frequencies, the fit is not adequate in this region.

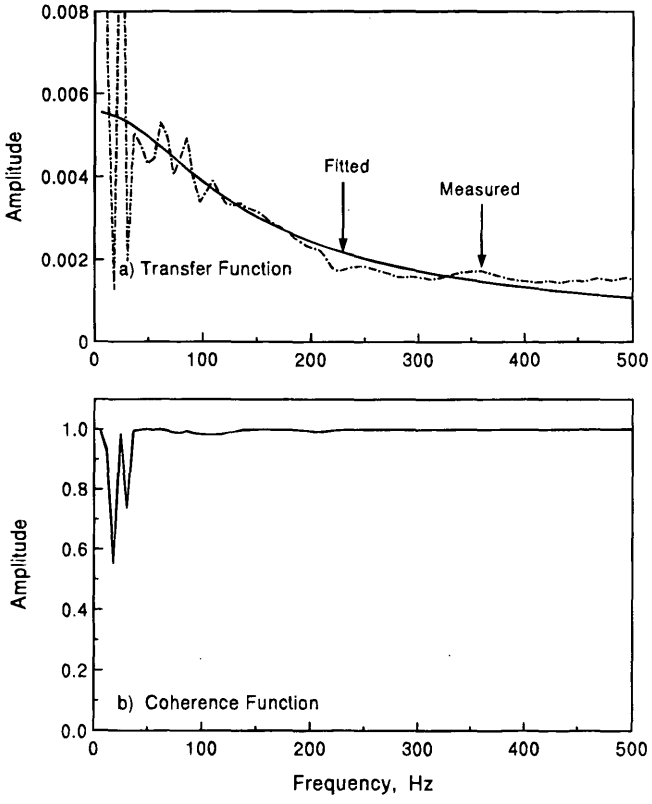

FIGURE 2 Typical spectral functions used in IR test.

The shear modulus of subgrade, G, is calculated from:

$$G = (1 - \nu) / [2L A_o I_s S_z] \quad (1)$$

where

ν = Poisson's ratio of subgrade;
L = length of slab; and
A_o = static flexibility of slab (flexibility at $f = 0$).

The shape factor, S_z, has been developed by Dobry and Gazetas (*2*). The value of S_z is equal to 0.80 for a long flexible pavement.

I_s is a parameter that considers the effect of an increase in flexibility near the edges and corners of a slab. Parameter I_s is a function of the length and width of the slab, as well as the coordinates of the impact point relative to one corner. Depending on the size of the slab and the point of impact, the value of I_s can be as high as 6.

The damping ratio, which typically varies between 0 to 100 percent, is an indicator of the degree of the slab's resistance to movement. A slab that is in contact with the subgrade or contains a water-saturated void demonstrates a highly damped behavior and has a damping ratio of greater than 70 percent. A slab containing an edge void would demonstrate a damping ratio in the order of 10 to 40 percent. A loss of support located in the middle of the slab will have a damping ratio of 30 to 60 percent.

Spectral-Analysis-of-Surface-Waves (SASW) Method

The SASW method is a seismic method that can determine shear modulus profiles of pavement sections nondestructively.

The key point in the SASW method is the measurement of the dispersive nature of surface waves. A complete investigation of a site with the SASW method consists of collecting data, determining the experimental dispersion curve, and determining the stiffness profile (inversion process).

The set-up used for the SASW tests is depicted in Figure 1. All accelerometers and geophones are active. The transfer function and coherence function between pairs of receivers are determined during the data collection.

A computer algorithm utilizes the phase information of the transfer function and the coherence functions from several receiver spacings to determine a representative dispersion curve in an automated fashion (*3*). The dispersion curves obtained from all receiver spacings from a site is shown in Figure 3(*a*). A curve is fitted to this data to obtain the "fitted-measured dispersion curve." This idealized curve is representative of the raw data.

The last step is to determine the elastic modulus of different layers, given the dispersion curve. A recently developed automated inversion process (*4*) determines the stiffness profile of the pavement section. This fitted curve is used in the inversion process. The modulus profile at the example site is shown in Figure 3(*b*). To ensure that the inversion process is successful, the fitted-measured dispersion curve is compared with the theoretical dispersion curve (obtained from the Young's modulus profile shown in Figure 3(*b*)). This comparison is depicted in Figure 3(*a*). The theoretical (labeled "from inverted model" in the figure) and experimental data (labeled "L1-norm fitted" in the figure) compare favorably.

Ultrasonic-Surface-Wave Method

The ultrasonic-surface-wave method is an offshoot of the SASW method. The major distinction between these two methods is that in the ultrasonic-surface-wave method the properties of the top paving layer can be easily and directly determined without a complex inversion algorithm. To implement the method, the high-frequency source and accelerometers A2 and A3 (see Figure 1) are utilized.

Up to a wavelength approximately equal to the thickness of the uppermost layer, the velocity of propagation is independent of wavelength. Therefore, if one simply generates high-frequency (short-wavelength) waves, and if one assumes that the properties of the uppermost layer are uniform, the shear modulus of the top layer, G, can be determined from

$$G = \rho\,[(1.13 - 0.16\nu)\,(m/360D)]^2 \qquad (2)$$

Parameter m (degree/Hz) is the least-squares fit slope of the phase of the transfer function in the high-frequency range.

A typical phase spectrum is shown in Figure 4(*a*). The phase oscillates on a radius between π and $-\pi$ radians (180 and -180 degrees). This is the standard method of presenting phase data, because the detailed variation in the data can be observed in a small space.

The coherence function associated with this record is shown in Figure 4(*b*). The coherence is almost equal to 1, up to a frequency of 35 or 40 kHz. Above the frequency of 35 kHz, the data are of low quality and are not usable.

The frequency of 35 kHz for this experiment corresponds to a wavelength of less than 38 mm. Shorter wavelengths can be investigated using Accelerometer 1 and Accelerometer 2 (which are spaced 75 mm apart). One physical limitation is the aggregate size. Wavelengths shorter than the maximum aggregate size probably do not follow the laws of wave propagation in solid medium.

The shear modulus of the top layer was obtained using a complex-valued curve-fitting process with the coherence as the weighing function (*3*). The results are shown in Figure 4(*a*). The actual and fitted curves compare quite favorably up to a frequency of 30 kHz. In the next step, the phase is "unwrapped;" that is, the appropriate number of cycles is added to each phase. The unwrapped phase for the "wrapped" phase shown in Figure 4(*a*) is shown in Figure 4(*c*). The slope of the line, which is basically constant with frequency, is used in Equation 2.

Ultrasonic-Compression-Wave-Velocity Measurement

Once the compression wave velocity of a material is known, its Young's modulus can be readily determined. The same set-up used to perform the SASW tests can be used to measure compression wave velocity of the upper layer of pavement.

The body wave energy present in a seismic record generated using the set-up shown in Figure 1 is small, and for all practical purposes it does not contaminate the SASW results. However, compression waves travel faster than any other type of seismic wave, and are detected first on seismic records.

Typical travel times, expanded to demonstrate the arrival of the compression waves, are shown in Figure 5. The arrows in each

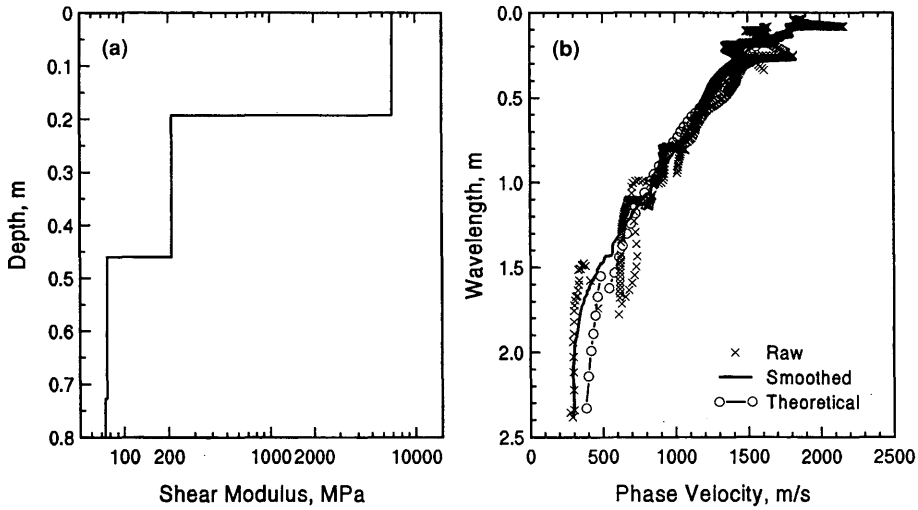

FIGURE 3 Typical results from SASW tests.

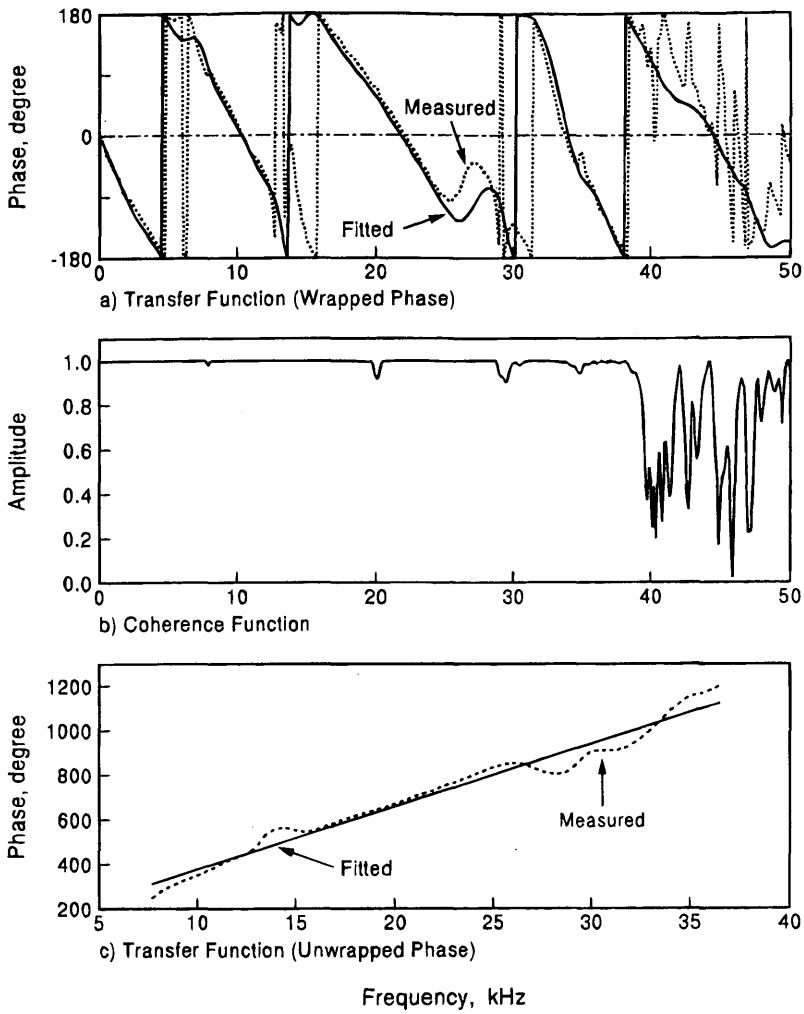

FIGURE 4 Typical spectral functions used in ultrasonic-surface-wave test.

record correspond to the arrival of these waves. Typically, Accelerometers 3 and 4 record the arrival of energy most consistently. The determination of the arrival of compression waves from Accelerometers 1 and 3 are typically not possible because of the closeness of the sensors to the source.

An automated technique for determining the arrival of compression waves has been developed. Times of first arrival of compression waves are measured by triggering on an amplitude range within a time window (*5*).

Impact-Echo Method

The impact-echo method can effectively locate defects, voids, cracks, and zones of deterioration within concrete.

The high-frequency source and accelerometer A1 are used, and possibly A2 as well (see Figure 1). Once the compression wave velocity of concrete, V_p, is known, the depth-to-reflector, T, can be determined from

$$T = V_p / 2f \quad (3)$$

where f is the resonant (return) frequency obtained by transforming the deformation record into the frequency domain.

A typical frequency-response spectrum for a site is shown in Figure 6(*a*). The major peak (at about 10 kHz) corresponds to the thickness of the layer and is called the return (resonant) frequency, which is input in Equation 3.

The coherence function is shown in Figure 6(*b*). In general, the data collected with the device have no incoherent noise, except at several isolated frequencies.

CASE STUDIES

Two case studies are incorporated here for demonstration purposes. Numerous other ones can be found in Nazarian et al. (*1*).

Case 1: Rigid Pavement

A jointed concrete pavement section was tested to determine the existence of voids and loss of support in the pavement. The pave-

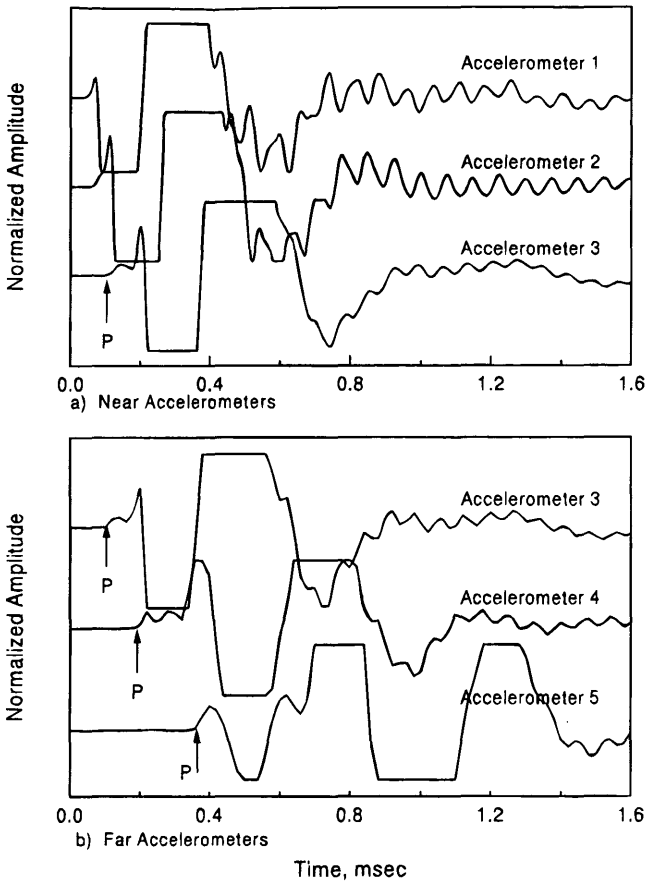

FIGURE 5 Typical amplified signals used in ultrasonic-body-wave test.

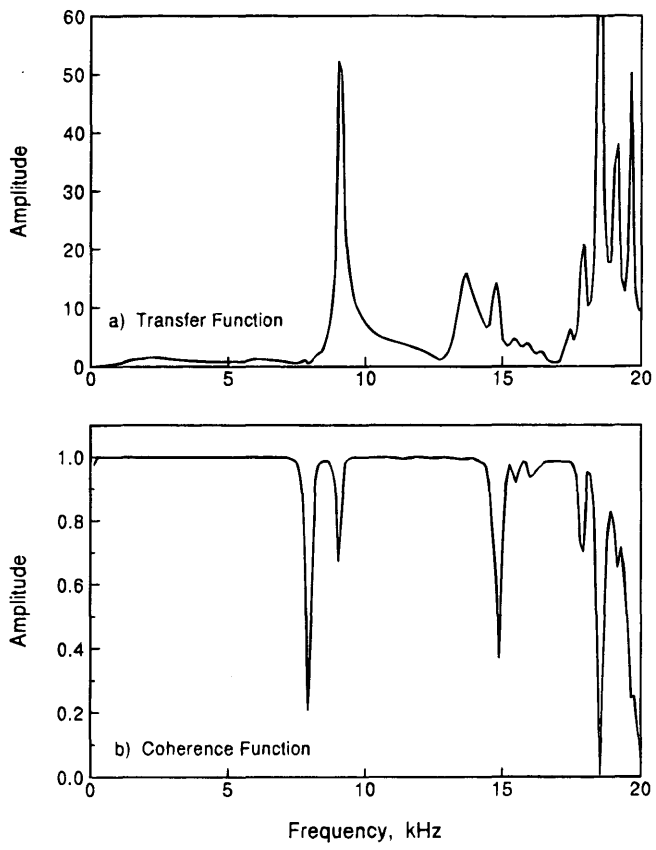

FIGURE 6 Typical spectral functions used in impact-echo test.

ment section at the site consisted of 225 mm jointed-concrete pavement over a cement-treated base.

The Portland cement concrete (PCC) slabs were 9 m long and 3.6 m wide. Twelve slabs (13 joints numbered 1 through 13) were tested. Three points were tested at each slab. The three points were located at 15 cm east and west of each joint and in the middle of each slab.

The IR test was used to detect voids and loss of support. The resulting moduli of subgrade and damping ratios are shown in Figure 7. The mean subgrade modulus is about 175 MPa. This indicates an above-average subgrade material. This section is in good condition, which is to be expected because the section was recently rehabilitated.

The data presented here indicate the need to inspect and maintain the approach side of each joint for possible voids, especially for Joints 2, 3, 5, 6, and 9. The two slabs between Joints 11 and 13 are in very bad condition and should be repaired. These recommendations are consistent with the condition of the pavement.

Most of the damping ratios shown in Figure 7(*b*) are above the critical damping ratio, indicating either water saturation of voids or good contact at the interface of the concrete and base layer. As indicated before, the water-saturated voids and intact locations are both highly damped; however, the intact points exhibit substantially higher moduli of subgrade.

To verify these results, five epoxy core holes were installed at the section, as marked in Figure 7. Points 2, 4, and 5 were selected as areas where voids were suspected. These three core points validated the SPA prediction that they were water-saturated voids (low modulus of subgrade, high damping ratio). Upon coring, the holes filled with water almost instantaneously. The other two cores were selected as intact concrete. Points 1 and 3 proved to be on relatively dry and intact subgrade.

The values of Young's and shear moduli of the slab are shown in Figure 8(*a*). Only the properties from the middle of the slab are shown here. Some variation in the results can be attributed to the variability in the material properties and also to some variability in data interpretation. In most cases, the material properties vary because both methods measure consistently lower or higher for the same points. In the middle of Slab 3, similar values for the shear and Young's moduli are reported; the reason for this discrepancy is the existence of a crack between the source and the accelerometer used to measure the compression wave velocity.

In general, the average Young's and shear moduli are 33 GPa and 15 GPa, respectively. These values represent average-quality concrete. From the average shear and Young's moduli, the average Poisson's ratio is about 0.14. This is an acceptable value for Poisson's ratio of concrete.

The measurements of the thickness of the PCC are shown in Figure 8(*b*). At the two core holes, the actual thicknesses of concrete is about 230 mm. The two points on Slabs 11 and 12 that exhibit smaller thickness are in the area where the concrete requires repair. The reason for the thinness of Slab 8 is not known.

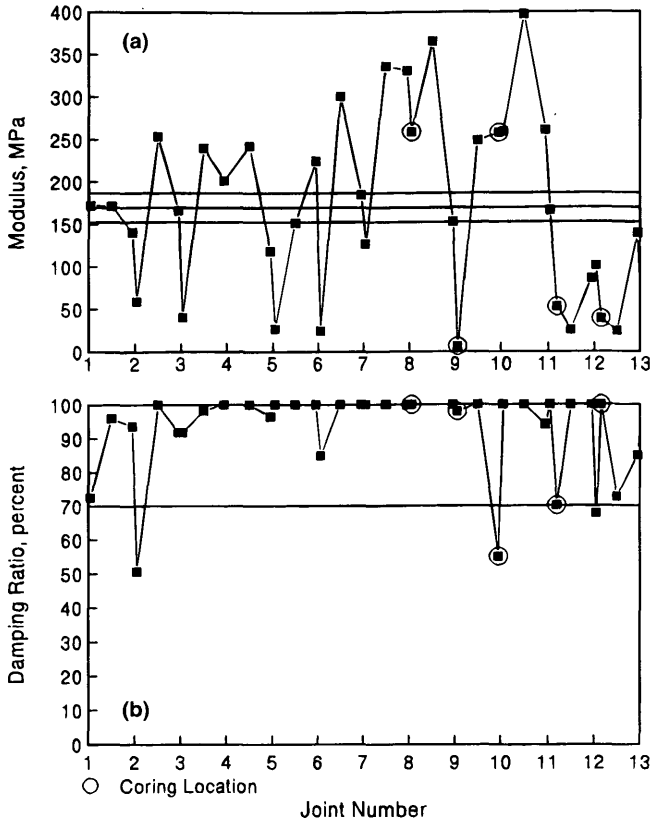

FIGURE 7 Variation in parameters measured with IR method at the rigid pavement site.

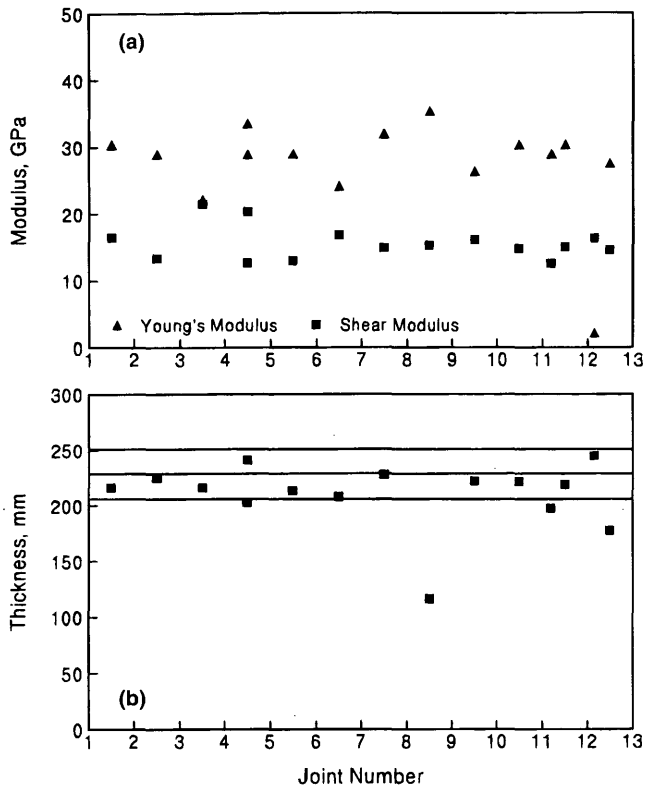

FIGURE 8 Variations in moduli and thickness of PCC at the rigid pavement site.

This case study demonstrates that the SPA is capable of evaluating rigid pavements for the existence of voids and loss of support in both dry and saturated conditions. At the five points where ground truth is available, the predictions were accurate.

Case 2: Flexible Pavement

The typical pavement cross section of this site consisted of 210 mm of AC over 250 mm of granular base over a corrodible sandy subgrade. A 1300-m section of the highway was selected and tested at 30-m intervals. The FWD device was used 3 weeks after the SPA tests were completed. These tests determine the softening of the subgrade as a result of the penetration of moisture.

The deflections for a nominal load of 40 kN are shown in Figure 9. A large variation in the deflection basins can be observed, possibly indicating the variability in the overall stiffness of the section. The variations in the deflections also may result from variations in the thickness or stiffness of the layers.

The modulus values obtained at the site from BISDEF are not included because back-calculation was not successful. At all points, the modulus of the AC was back-calculated as the upper prescribed range of 17.5 GPa, and the base modulus was always equal to 35 MPa (the lower range assigned to the material for the back-calculation). This may be partly the result of the dynamic interaction between the bedrock and the FWD. A large portion of the site was in a cut section.

The IR test was used to determine the effects of moisture variation in the base and subgrade. The IR test was utilized to determine the overall variation in stiffness, and the SASW method was employed for more thorough analysis.

The measurements of the modulus of the subgrade soil are shown in Figure 10. The pavement in the range of −50 m to −80 m corresponded to a saturated base and subgrade. The rest of the section seemed to be in reasonably good condition. However, the data indicate some potential problems in the 200-m to 350-m section. The level of water in a ditch on the side of the road was rather high in this area.

The results from the SASW tests are summarized in Table 1. These tests were carried out at some of the core locations; therefore, they do not correspond to test results described above. The moduli of the AC layer are relatively constant. The base moduli are similar, except for the two points tested at −84 m and −54 m. The base material at the −84 m location was saturated, and water was seeping to the pavement surface. The point tested at −54 m was also wet. The subgrade moduli are rather high for points 360 m and 900 m, and are representative of most of the pavement section. The test point at 270 m corresponds to the area that the IR tests diagnosed as soft. At this point, the subgrade is quite soft, whereas the AC and base layers are in good condition.

The water contents (also recorded in Table 1) were obtained in the field with a pan-dry oven. As indicated, the base at −84 m has the highest water content and also the lowest modulus. The two points located at 360 m and −54 m exhibit similar water content;

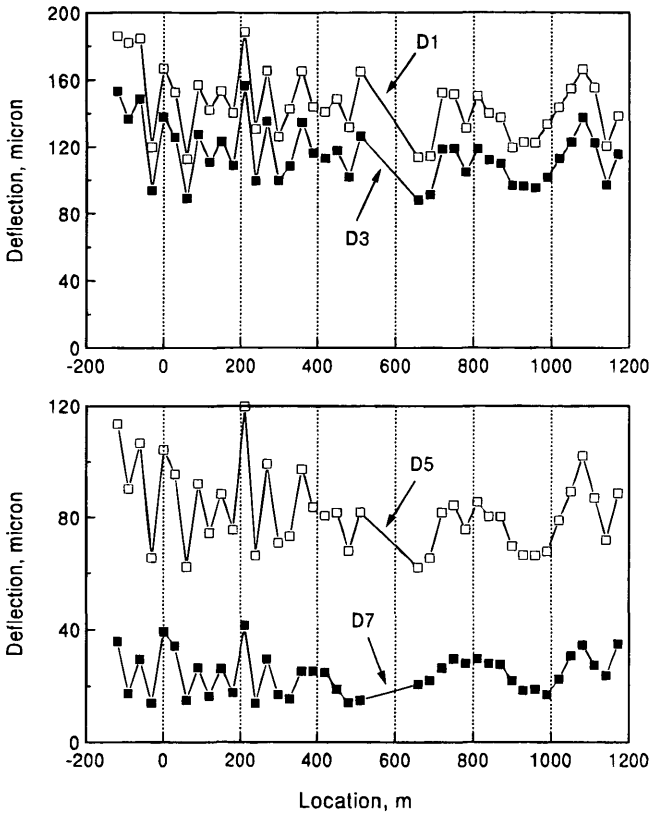

FIGURE 9 Variation in deflection basins at the flexible pavement site.

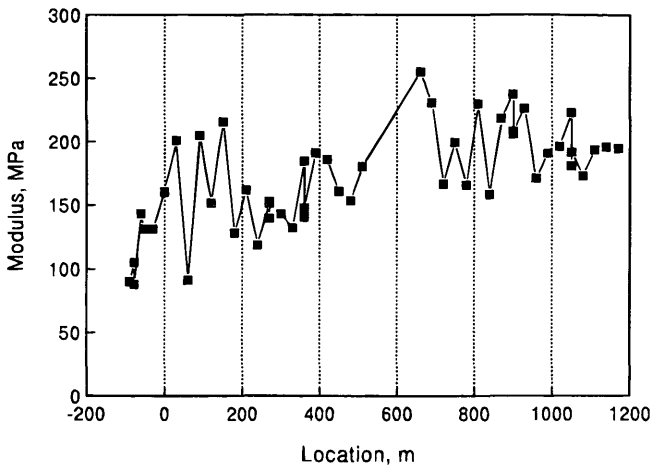

FIGURE 10 Variation in modulus of subgrade soil from IR tests at the flexible pavement site.

however, the moduli of these two points are significantly higher than that of point −84 m. Point 360 m, with base moisture similar to point −84 m, is significantly stiffer than point −84 m. Both independent tests (IR and SASW) concur that point −84 m is not as stiff as point −54 m or point 360 m. Based on engineering intuition, the pavement structure at point −84 m should therefore be softer than the other points. Points −84 m and −54 m are located in a rock cut, whereas point 360 m was almost in a fill section. Therefore, the dynamic interaction would affect the deflections from FWD, and the SPA results could not be verified.

Establishing a relationship between the modulus and water content, without considering other factors such as the type of the base and subgrade materials, optimum water content for the base and subgrade, and the period of time that the material is exposed to the moisture, may not be appropriate.

The values of the shear modulus of the asphalt concrete layer are shown in Figure 11(*a*). The pavement in locations around 600 m was not tested because there was a bridge. Moduli are clustered at two levels. Between locations 0 m and 600 m, the moduli are higher than the rest of the section, because of the temperature sensitivity of the AC layer. The 600-m section (between 0 m and 600 m) was tested in the early morning when the pavement was cold (ambient temperature of −2°C), and the other sections were tested later, when the sun had been out, raising ambient temperature to 22°C.

The values of Young's modulus as determined from the ultrasonic-body-wave tests are shown in Figure 11(*b*). The same clustering of moduli can be seen in the results of this test as well;

TABLE 1 Shear Modulus Profiles Obtained at the Flexible Pavement Site

Location, m	Shear Modulus, MPa			Water Content, percent		FWD Deflection*, micron	
	AC	Base	Subgrade	Base	Subgrade	D1	D7
-84	7530	78	45	6.2	14.4	179**	17
-54	6433	127	89	5.7	--	182**	29
270	6944	210	77	4.0	11.8	160	29
360	8486	214	150	6.0	14.1	160	25
900	7960	205	136	4.1	15.7	112	21

* Deflections, which are reported for a nominal load of 40 KN, should be considered with caution, since a stiff layer existed under the pavement at variable depths.

** FWD tests were not carried out at this location. The closest point tested is reported.

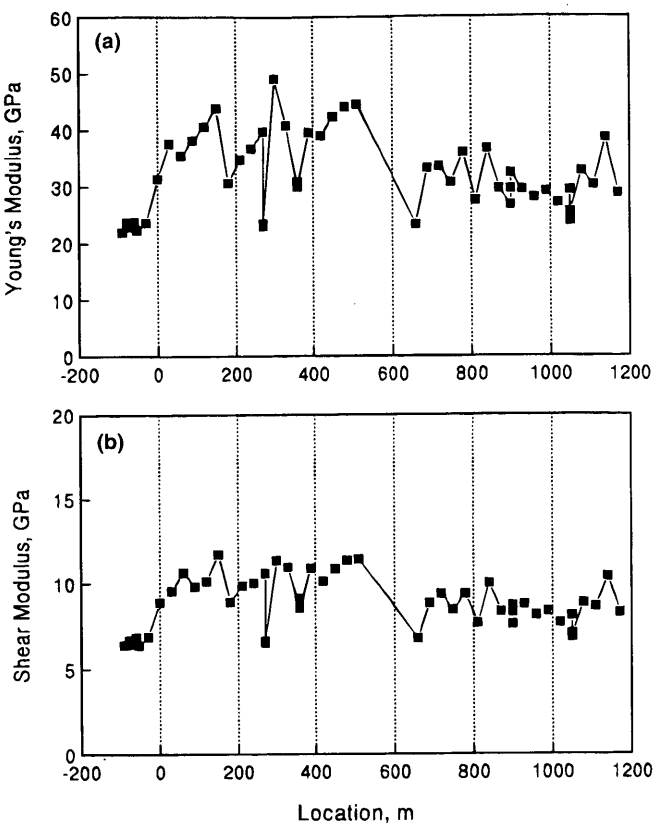

FIGURE 11 Variations in moduli of AC at the flexible pavement site.

the two independent testing methodologies yield relatively similar results. From the shear and Young's moduli, Poisson's ratio is in the range of 0.29 to 0.35, which is quite reasonable. In general, this case study clearly shows the potential, accuracy, and the robustness of the SPA.

CONCLUSIONS

Based on the information presented, it can be concluded that the new SPA nondestructive testing device is useful for pavement evaluation, and that the SPA can easily, accurately, and repeatably collect information about the condition of pavements.

ACKNOWLEDGMENTS

This work was funded by the Strategic Highway Research Program under Project H-104B. The financial and technical assistance of that organization is appreciated.

In addition, the support and financial backing of the Texas Department of Transportation should be mentioned. Without the trust and support of that organization, this project could not have been completed.

REFERENCES

1. Nazarian, S., R. D. Baker, and K. Crain. *Development and Testing of a Seismic Pavement Analyzer.* Research Report SHRP-H-375. Strategic Highway Research Program, TRB, National Research Council, Washington, DC, 1993.
2. Dobry, R., and G. Gazetas. Dynamic Response of Arbitrary Shaped Foundations. *Journal of Geotechnical Engineering*, Vol. 112, No. 2, 1986, pp. 109–135.
3. Nazarian, S., and M. Desai. Automated Surface Wave Testing: Field Testing. *Journal of Geotechnical Engineering*, Vol. 119, No. GT7, 1993, pp. 1094–1112.
4. Yuan, D., and S. Nazarian. Automated Surface Wave Testing: Inversion Technique. *Journal of Geotechnical Engineering*, Vol. 119, No. GT7, 1993, pp. 1112–1126.
5. Willis, M. E., and M. N. Toksoz. Automatic P and S Velocity Determination from Full Wave Form Digital Acoustic Logs. *Geophysics*, Vol. 48, No. 12, 1983, pp. 1631–1644.

Publication of this paper sponsored by Committee on Pavement Monitoring, Evaluation, and Data Storage.